arXiv:hep-ph/0212072v1 4 Dec 2002

Calculation of radiative corrections to the effect of parity nonconservation in heavy atoms

A.I.Milstein*
Budker Institute of Nuclear Physics, 630090 Novosibirsk, Russia

O.P.Sushkov†
School of Physics, University of New South Wales, Sydney 2052, Australia

I.S.Terekhov‡
Novosibirsk University, 630090 Novosibirsk, Russia

(Dated: February 7, 2008)

We calculate the self-energy and the vertex radiative corrections to the effect of parity nonconservation in heavy atoms. The sum of the corrections is of the form $\mathcal{A}\ln(\lambda_C/r_0)+\mathcal{B}$, where $\mathcal{A}$ and $\mathcal{B}$ are functions of $Z\alpha$, and λ_C and r_0 are the Compton wavelength and the nuclear radius, respectively. The function $\mathcal{A}$ is calculated exactly in $Z\alpha$ and the function $\mathcal{B}$ is calculated in the leading order. In the leading order $\mathcal{A}\propto\alpha(Z\alpha)^2$ and $\mathcal{B}\propto\alpha(Z\alpha)$. The sum of the corrections is -0.85% for Cs and -1.48% for Tl. Using these results we have performed analysis of the experimental data on atomic parity nonconservation. The values obtained for the nuclear weak charge, $Q_W=-72.81(28)_{exp}(36)_{theor}$ for Cs and $Q_W=-116.8(1.2)_{exp}(3.4)_{theor}$ for Tl, agree with predictions of the standard model within 0.6σ. As an application of our approach we have also calculated dependence of the Lamb shift on the finite nuclear size.

PACS numbers: 11.30.Er, 31.30.Jv, 32.80.Ys

I. INTRODUCTION

Atomic parity nonconservation (PNC) has now been measured in bismuth [1], lead [2], thallium [3], and cesium [4]. Analysis of the data provides an important test of the standard electroweak model and imposes constraints on new physics beyond the model, see Ref. [5]. The analysis is based on the atomic many-body calculations for Tl, Pb, and Bi [6] and for Cs [7, 8] (see also more recent Refs. [9, 10]). Both the experimental and the theoretical accuracy is best for Cs. Therefore, this atom provides the most important information on the standard model in the low-energy sector.

In the many-body calculations [6, 7, 8] the Coulomb interaction between electrons was taken into account, while the magnetic interaction was neglected. The contribution of the magnetic (Breit) electron-electron interaction was calculated in the papers [11, 12]. It proved to be much larger than a naive estimate, and it shifted the theoretical prediction for PNC in Cs.

Radiative correction to the nuclear weak charge due to renormalization from the scale of the W-boson mass down to zero momentum has been calculated long time ago, see Refs. [13, 14]. This correction is always included in the analysis of data. However, another important class of radiative corrections was omitted in the analysis of atomic PNC. This fact has been pointed out in work [15] that demonstrated that there are corrections $\sim Z\alpha^2$ caused by the collective electric field of the nucleus. Here Z is the nuclear charge and α is the fine structure constant. The simplest correction of this type is due to the Uehling potential. It has been calculated numerically in Ref. [16] and analytically in our paper [17]. In that paper [17] we have also analyzed the general structure of the radiative corrections caused by the collective electric field. It has been shown that, as well as the usual perturbative parameter $Z\alpha$, there is an additional parameter $\ln(\lambda_C/r_0)$ where λ_C is the electron Compton wavelength and r_0 is the nuclear radius.

In the present work we consider radiative corrections to the atomic PNC effect due to electron self-energy and vertex. The total correction is of the form $\mathcal{A}\ln(\lambda_C/r_0)+\mathcal{B}$, where $\mathcal{A}$ and $\mathcal{B}$ are functions of $Z\alpha$. We calculate the function $\mathcal{A}$ exactly in $Z\alpha$ and the function $\mathcal{B}$ in the leading order. In the leading order $\mathcal{A}\propto\alpha(Z\alpha)^2$ and $\mathcal{B}\propto\alpha(Z\alpha)$. Results of the leading order calculations have been reported in Ref. [18]. Using results of our calculations we reanalyze

---

*Email:A.I.Milstein@inp.nsk.su
†Email:sushkov@phys.unsw.edu.au
‡Email:I.S.Terekhov@inp.nsk.su

the experimental data for atomic PNC. Agreement with the standard model is excellent.

As an application of our approach we have also calculated the dependence of the Lamb shift on the finite nuclear size. Agreement of our analytical formula with results of previous computations [19, 20] is perfect. Structure of the present paper is following. In Sec. II we discuss the general structure of the PNC amplitude. In Secs. III and IV we calculate logarithmic parts of the self-energy and the vertex contributions, respectively. In Sec.V we calculate the linear in $Z\alpha$ correction to the PNC amplitude. In Sec. VI we calculation the dependence of the Lamb shift on the finite nuclear size. Finally in Sec. VII we analyze experimental data on atomic PNC and present our conclusions.

II. GENERAL STRUCTURE OF THE PNC AMPLITUDE

The strong relativistic enhancement is a special property of the atomic PNC effect. The relativistic enhancement factor is proportional to $R \sim (\lambda_C/Z\alpha r_0)^{2(1-\gamma)}$, where $\gamma = \sqrt{1-(Z\alpha)^2}$. The factor is $R \approx$3 for Cs and $R \approx 9$ for Tl, Pb, and Bi [21]. For nuclear radius we use the formula

$$r_0 \approx 1.1\ A^{1/3}\ fm \approx 1.5\ Z^{1/3}\ fm. \tag{1}$$

The relativistic enhancement factor R is divergent at $r_0 \to 0$. This makes the relativistic behavior of PNC very much different from the behavior of the hyperfine structure. The logarithmic enhancement of radiative corrections mentioned above is closely related to the existence of the factor R. The Feynman diagram for the leading contribution to the PNC matrix element between $p_{1/2}$ and $s_{1/2}$ states as well as diagrams for one loop radiative corrections are shown in Fig.1(a) and Fig.1(b-f), respectively. Strictly speaking the diagrams in Figs.1(b-f) are not quite well defined because they describe the matrix element between states with different energies, so it is not clear what energy corresponds to the external legs. However the external legs describe states of the external atomic electron, say $6s$, $6p$, $7s$,... states in Cs, that have very small binding energies of the order of $m\alpha^2$ (m is the electron mass). Therefore, the uncertainty in the definition of the diagrams appears only in the order $\alpha^3(Z\alpha)$ which we do not consider in the present work. The diagram Fig.1(b) corresponds to a modification of the electron wave function because of the vacuum polarization. This correction calculated analytically in Ref. [17] reads

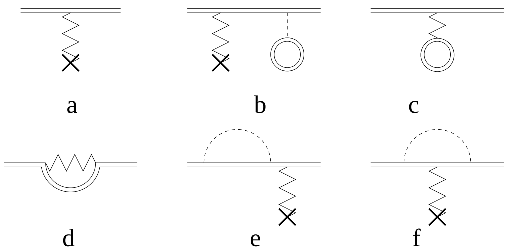

FIG. 1: *(a) Leading contribution to the PNC matrix element. (b-f) One loop radiative corrections. The double line is the exact electron Green's function in the Coulomb field of the nucleus, the cross denotes the nucleus, the zigzag and the dashed lines denote Z-boson and photon, respectively.*

$$\delta_b = \alpha \left(\frac{1}{4} Z\alpha + \frac{2(Z\alpha)^2}{3\pi\gamma} \left[\ln^2(b\lambda_C/r_0) + f \right] \right), \tag{2}$$

where $b = \exp(1/(2\gamma) - C - 5/6)$, $C \approx 0.577$ is the Euler constant, and $f \sim 1$ is some smooth function of $Z\alpha$ independent of r_0. Hereafter we denote by δ the relative value of the correction. So, Eq. (2) represents the ratio of diagrams Fig.1(b) and Fig.1(a).

The renormalization of the nuclear weak charge Q_W from the scale of the W-boson mass down to $q = 0$ was performed in Refs. [13, 14]. However, as has been pointed out in Ref. [17], atomic experiments correspond to $q \sim 1/r_0 \sim 30$MeV, see also Ref. [22]. The correction due to renormalization from $q = 0$ to $q = 1/r_0$ is described by diagrams Fig.1(c) and Fig.1(d). It has the form [17]

$$\delta_{cd} = \frac{4\alpha Z}{3\pi Q_W} (1 - 4\sin^2\theta_W) \ln(\lambda_C/r_0) \sim -0.1\%, \tag{3}$$

where θ_W is the Weinberg angle, $\sin^2\theta_W \approx 0.2230$, see Ref. [5].

Diagrams Fig.1(e) and Fig.1(f) correspond to the contributions of the electron self-energy operator and the vertex operator, respectively. Neither of these diagrams is invariant with respect to the gauge transformation of the electromagnetic field. However, their sum is gauge invariant. It has been demonstrated in Ref. [17] that the correction $\delta_e + \delta_f$ is of the form

$$\delta_{ef} = \delta_e + \delta_f = \mathcal{A} \ln(b\lambda_C/r_0) + \mathcal{B} \quad , \tag{4}$$

where $\mathcal{A}$ and $\mathcal{B}$ are functions of $Z\alpha$, and the constant b is defined after Eq.(2). In the leading approximation in the parameter $Z\alpha$ the functions are, $A = (a_2/\pi)\ \alpha(Z\alpha)^2$ and $B = a_1\ \alpha(Z\alpha)$. In the work [17] we have also obtained preliminary estimates for the coefficients a_1 and a_2. The estimates were based on an assumption of analogy between the polarization operator and the self-energy operator. This assumption and hence the preliminary estimates proved to be wrong. In the present work we calculate the coefficients a_1 and a_2 exactly. Moreover, we also calculate the function $\mathcal{A}$ *exactly* in the parameter $Z\alpha$. The functions $\mathcal{A}$ and $\mathcal{B}$ are calculated by different methods. For calculation of $\mathcal{A}$ we use electron Green's functions in the Coulomb field at $r \ll \lambda_C$ and the Feynman gauge. The non-logarithmic term $\mathcal{B}$ we find using the effective operator method and the Fried-Yennie gauge [23]. The method is based on calculation of the low-energy scattering amplitude in the potential induced by Z-boson exchange.

Let us consider the PNC matrix element between $p_{1/2}$ and $s_{1/2}$ states. The wave function of the external electron is of the form

$$\psi(\boldsymbol{r}) = \begin{pmatrix} F(r)\Omega \\ iG(r)\tilde{\Omega} \end{pmatrix} \quad , \tag{5}$$

where Ω and $\tilde{\Omega} = -(\boldsymbol{\sigma} \cdot \boldsymbol{n})\Omega$ are spherical spinors[24]. Calculation of the weak interaction matrix element in the leading approximation gives [21]

$$< p_{1/2}|(2\sqrt{2})^{-1} G_F Q_W \rho(r)\gamma_5|s_{1/2} >_0 = M_0 \propto (F_s G_p - G_s F_p)|_{r=r_0}. \tag{6}$$

Here G_F is the Fermi constant, and $\rho(r)$ is the density of the nucleus normalized as $\int \rho(r) d\boldsymbol{r} = 1$. At small distances, $r \ll Z\alpha\lambda_C$, the electron mass can be neglected compared to the Coulomb potential energy, and solution of the Dirac equation for the radial wave functions reads

$$F = N r^{\gamma-1}, \quad G = N\frac{Z\alpha}{\kappa - \gamma} r^{\gamma-1}, \tag{7}$$

where $\kappa = -1$ for $s_{1/2}$-state and $\kappa = 1$ for $p_{1/2}$-state, and N is some constant dependent on the wave-function behavior at large distances ($r \sim a_B$) [21]. Calculation of the constant N is a very complex many-body problem, see Refs.[7, 8]. Fortunately, the constant is cancelled out from the relative correction which we consider. Due to Eq. (7) the matrix element (6) is divergent at $r_0 \to 0$, $M_0 \propto r_0^{2\gamma-2}$. This leads to the strong relativistic enhancement factor mentioned above.

The correction to M_0 related to the diagram Fig.1(e) can be obtained as follows. The electron self-energy operator $\boldsymbol{\Sigma}$ being substituted to the Dirac equation, $m \to m + \boldsymbol{\Sigma}$, leads to the Lamb shift of energy levels and to the modification of electron wave functions, see, e.g., Ref. [24]. The wave function modification influences the matrix element of the weak interaction. We will call the Dirac equation with account of the self-energy operator the modified Dirac equation.

It is convenient to search for solution of the modified Dirac equation in the form (5) with substitutions $F \to F(1 + F^{(1)})$, $G \to G(1 + G^{(1)})$, where $F^{(1)}$ and $G^{(1)}$ are corrections due to the self energy. Using this form in Eq.(6) together with (7) we obtain the following relative correction to the PNC matrix element

$$\delta = M^{(1)}/M^{(0)} = \left\{ \frac{1+\gamma}{2} \left[F_s^{(1)} + G_p^{(1)*} \right] + \frac{1-\gamma}{2} \left[G_s^{(1)} + F_p^{(1)*} \right] \right\} \Big|_{r=r_0} \quad . \tag{8}$$

Similar to Eqs.(5),(7), we represent the self-energy term in the Dirac equation $\Psi^{\Sigma} = \boldsymbol{\Sigma}\psi$ as

$$\Psi^{\Sigma} = \begin{pmatrix} F^{(2)}\Omega \\ iG^{(2)}\dfrac{Z\alpha}{\kappa-\gamma}\tilde{\Omega} \end{pmatrix} r^{\gamma-2} \quad . \tag{9}$$

In the next Section we will show that $F^{(2)}$ and $G^{(2)}$ are independent of r at $r \ll Z\alpha\lambda_C$. The functions $F^{(1)}$ and $G^{(1)}$ satisfy the following equations

$$\begin{aligned} \frac{1}{\gamma+\kappa}\frac{\partial F^{(1)}}{\partial x} - F^{(1)} + G^{(1)} &= -\frac{1}{Z\alpha} G^{(2)} \\ \frac{1}{\kappa-\gamma}\frac{\partial G^{(1)}}{\partial x} - F^{(1)} + G^{(1)} &= -\frac{1}{Z\alpha} F^{(2)} \quad , \end{aligned} \tag{10}$$

where $x = -\ln(r/\lambda_C)$. The solution of Eqs. (10) reads

$$\begin{aligned} F^{(1)} &= \frac{Z\alpha x}{2\gamma}\,[G^{(2)} - F^{(2)}] + \frac{1}{4Z\alpha\gamma}\,[(\kappa+\gamma)G^{(2)} - (\kappa-\gamma)F^{(2)}] + a\,, \\ G^{(1)} &= \frac{Z\alpha x}{2\gamma}\,[G^{(2)} - F^{(2)}] - \frac{1}{4Z\alpha\gamma}\,[(\kappa+\gamma)G^{(2)} - (\kappa-\gamma)F^{(2)}] + a\,, \end{aligned} \tag{11}$$

where a is some constant. Note that in the leading logarithmic approximation (the terms proportional to x) $F^{(1)} = G^{(1)}$. Substituting (11) into Eq.(8), we find

$$\delta_e \;=\; \frac{Z\alpha L}{2\gamma}\left[G_s^{(2)} + G_p^{(2)*} - F_s^{(2)} - F_p^{(2)*}\right] + const. \tag{12}$$

Here $L = \ln(b\lambda_C/r_0)$, and by *const* we denote $Z\alpha$-dependent terms that do not contain the large logarithm L. It will be shown below that $F_p^{(2)} = -G_s^{(2)}$ and $G_p^{(2)} = -F_s^{(2)}$. Hence, the correction δ_e is of the form

$$\delta_e = \frac{Z\alpha}{\gamma}\mathrm{Re}\left[G_s^{(2)} - F_s^{(2)}\right] L + const\,. \tag{13}$$

We will demonstrate that $G_s^{(2)}$ and $F_s^{(2)}$ are odd functions of $Z\alpha$. Therefore, the factor before the logarithm L is an even function of $Z\alpha$ and hence the leading term of $Z\alpha$-expansion of this function is proportional to $\alpha(Z\alpha)^2$. The *const* in Eq.(13) can be determined from the condition that the correction to the wave function is orthogonal to the solution of the non-modified Dirac equation. Therefore, the main contribution to the *const* comes from the distances $r \sim \lambda_C$, and hence the leading term of $Z\alpha$-expansion of the *const* is proportional to $\alpha(Z\alpha)$. The correction δ_f corresponding to the diagram in Fig.1(f) has the same properties as δ_e.

III. LOGARITHMIC CONTRIBUTION OF THE SELF-ENERGY OPERATOR

At $r \ll \lambda_C$ one can neglect the electron mass in the propagator and write down $\Psi^\Sigma = \boldsymbol{\Sigma}\psi$ as

$$\Psi^\Sigma(\boldsymbol{r}_2) = 2\alpha \int\limits_{-\infty}^{\infty} d\epsilon \int d\boldsymbol{r}_1 \gamma_\mu \mathcal{G}(\boldsymbol{r}_2, \boldsymbol{r}_1|\, i\epsilon)\gamma^\mu\, D(\boldsymbol{r}_2, \boldsymbol{r}_1|i\epsilon)\psi(\boldsymbol{r}_1) \quad , \tag{14}$$

where $\mathcal{G}$ is the electron Green's function in the Coulomb field, $g_{\mu\nu}D$ is the photon Green's function in the Feynman gauge. In (14) we have deformed the contour of integration over the energy ϵ in such a way that it coincides with the imaginary axis. According to the integral representation derived in [25], the Green's function is of the form

$$\begin{aligned} &\mathcal{G}(\boldsymbol{r}_2, \boldsymbol{r}_1|\, i\epsilon) = -\frac{i}{4\pi r_1 r_2}\sum_{l=1}^{\infty}\int\limits_0^{\infty} ds \exp\left[\,2iZ\alpha\lambda s - k(r_1 + r_2)\coth s\,\right] T\,, \\ &T = \gamma^0[1 - (\boldsymbol{\gamma n}_2)(\boldsymbol{\gamma n}_1)]\left[\lambda\frac{y}{2}I'_{2\nu}(y) - iZ\alpha\coth s\, I_{2\nu}(y)\right] B + \gamma^0[1 + (\boldsymbol{\gamma n}_2)(\boldsymbol{\gamma n}_1)]\lambda I_{2\nu}(y) A \\ &- \left[\frac{k(r_2 - r_1)}{2\sinh^2 s}(\boldsymbol{\gamma}, \boldsymbol{n}_1 + \boldsymbol{n}_2)B + \coth s(\boldsymbol{\gamma}, \boldsymbol{n}_2 - \boldsymbol{n}_1)A\right] I_{2\nu}(y)\,, \\ &y = \frac{2k\sqrt{r_1 r_2}}{\sinh s}\,, \quad A = l\frac{d}{dx}(P_l(x) + P_{l-1}(x)) \quad , \quad B = \frac{d}{dx}(P_l(x) - P_{l-1}(x)) \quad . \end{aligned} \tag{15}$$

Here $k = |\epsilon|$, $\lambda = \epsilon/k$, $\boldsymbol{n}_{1,2} = \boldsymbol{r}_{1,2}/r_{1,2}$, $x = \boldsymbol{n}_1 \cdot \boldsymbol{n}_2$, $P_l(x)$ is the Legendre polynomial, $I_{2\nu}$ is the modified Bessel function of the first kind, $\nu = \sqrt{l^2 - (Z\alpha)^2}$. Using relation

$$\int (\boldsymbol{n}_1 \times \boldsymbol{n}_2)\Phi(\boldsymbol{n}_1 \cdot \boldsymbol{n}_2) d\boldsymbol{n}_1 = 0 \quad ,$$

that is valid for arbitrary function $\Phi(x)$, and Eqs.(5), (7), (15), and(14) we get for s-wave

$$
\begin{aligned}
&\begin{pmatrix} F_s^{(2)} \\ G_s^{(2)} \end{pmatrix} = \frac{i\alpha r_2^{1-\gamma}}{\pi} \sum_{l=1}^{\infty} \sum_{\lambda=\pm 1} \int_0^{\infty} d\epsilon \int d\boldsymbol{r}_1\, r_1^{\gamma-2} \int_0^{\infty} ds q \exp\left[\, 2iZ\alpha\lambda s - k(r_1+r_2)\coth s\,\right] D(\boldsymbol{r}_2, \boldsymbol{r}_1|i\epsilon) \begin{pmatrix} f_s \\ g_s \end{pmatrix} , \\
&f_s = (1+x)B\left[\lambda\frac{y}{2}I'_{2\nu}(y) - iZ\alpha\coth s\, I_{2\nu}(y)\right] + (1-x)A\lambda I_{2\nu}(y) \\
&-\frac{iZ\alpha}{1+\gamma}\left[(1+x)B\frac{k(r_2-r_1)}{2\sinh^2 s} - (1-x)A\coth s\right] I_{2\nu}(y)\, , \\
&g_s = (1+x)(1-2x)B\left[\lambda\frac{y}{2}I'_{2\nu}(y) - iZ\alpha\coth s\, I_{2\nu}(y)\right] - (1-x)(1+2x)A\lambda I_{2\nu}(y) \\
&-\frac{iZ\alpha}{1-\gamma}\left[(1+x)B\frac{k(r_2-r_1)}{2\sinh^2 s} + (1-x)A\coth s\right] I_{2\nu}(y)\, . \qquad (16)
\end{aligned}
$$

Performing similar calculations for p-wave we find that $F_p^{(2)} = -G_s^{(2)}$ and $G_p^{(2)} = -F_s^{(2)}$. The explicit form of the photon Green's function D reads:

$$
D(\boldsymbol{r}_2, \boldsymbol{r}_1|i\epsilon) = -\frac{e^{-kR}}{4\pi R} \quad , \quad R = |\boldsymbol{r}_2 - \boldsymbol{r}_1| \quad . \qquad (17)
$$

Using Eqs.(16), (17),(13) as well as the substitution $\boldsymbol{r}_1 = r_2\boldsymbol{\rho}$, $\epsilon = E/r_2$ we obtain the following expression for the self-energy contribution to the function $\mathcal{A}$ (see, Eq.(4))

$$
\begin{aligned}
\mathcal{A}_{SE} &= -\frac{\alpha}{\pi^2\gamma}\sum_{l=1}^{\infty}\int_0^{\infty} dE \int \frac{d\boldsymbol{\rho}\,\rho^{\gamma-2}}{R}\int_0^{\infty} ds \exp\left[-E(\rho+1)\coth s - ER\right]\ (\Delta_1+\Delta_2) \quad , \\
\Delta_1 &= x(1+x)B\left[\frac{y}{2}I'_{2\nu}(y)(Z\alpha)\sin\phi - (Z\alpha)^2\cos\phi\coth s\, I_{2\nu}(y)\right] + (Z\alpha)(1-x^2)A\sin\phi\, I_{2\nu}(y)\, , \\
\Delta_2 &= \cos\phi\left[(1+x)B\frac{E\gamma(1-\rho)}{2\sinh^2 s} + (1-x)A\coth s\right] I_{2\nu}(y)\, . \qquad (18)
\end{aligned}
$$

Here $\phi = 2Z\alpha s$, $R = \sqrt{\rho^2 - 2\rho x + 1}$, $y = 2E\sqrt{\rho}/\sinh s$. It is obvious from this formula that $\mathcal{A}_{SE}$ is an even function of $Z\alpha$.

Equation (18) is not quite correct. The point is that the integrand in this equation has been derived for $\boldsymbol{r}_1 \neq \boldsymbol{r}_2$. However, there are also terms containing δ-function $\delta(\boldsymbol{r}_2 - \boldsymbol{r}_1)$ and derivative of this δ-function. To account for these terms we represent the self-energy operator as a series in powers of the Coulomb field of the nucleus, $\boldsymbol{\Sigma} = \boldsymbol{\Sigma}_0 + \boldsymbol{\Sigma}_1 + \boldsymbol{\Sigma}_2 + ...$, see Fig.2. The first two terms in the series, $\boldsymbol{\Sigma}_0$ and $\boldsymbol{\Sigma}_1$, require the ultraviolet regularization. It means that they contain terms with the δ-function and derivative of the δ-function. Both $\boldsymbol{\Sigma}_0$ and $\boldsymbol{\Sigma}_1$ depend on the parameter of the ultraviolet regularization. However, the contribution of $\boldsymbol{\Sigma}_{01} = \boldsymbol{\Sigma}_0 + \boldsymbol{\Sigma}_1$ to $\mathcal{A}_{SE}$ is independent of the regularization parameter because of the Ward identity. The operators $\boldsymbol{\Sigma}_n$ ($n \geq 2$) do not require any regularization. Note that Δ_1 in Eq.(18) corresponds to the contribution of the operators $\boldsymbol{\Sigma}_{2n+1}$, while Δ_2 corresponds to that of the operators $\boldsymbol{\Sigma}_{2n}$. Let us represent the self energy operator as $\boldsymbol{\Sigma} = \boldsymbol{\Sigma}_{01} + \boldsymbol{\Sigma}^{(n>1)}$. Corresponding contributions to the function $\mathcal{A}_{SE}$ are $\mathcal{A}_{SE}^{(01)}$ and $\mathcal{A}_{SE}^{(n>1)}$, hence

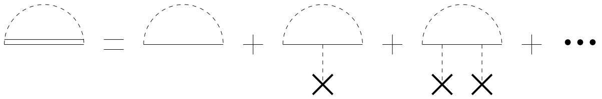

FIG. 2: *The electron self energy expanded in powers of the Coulomb field. The solid line is the free electron Green's function, the cross denotes the nucleus, and the dashed line denotes the photon.*

$$
\mathcal{A}_{SE} = \mathcal{A}_{SE}^{(01)} + \mathcal{A}_{SE}^{(n>1)}. \qquad (19)
$$

The terms singular at $\boldsymbol{r}_1 = \boldsymbol{r}_2$ contribute only to $\mathcal{A}_{SE}^{(01)}$. To overcome the problem with singularity we calculate $\mathcal{A}_{SE}^{(01)}$ using momentum representation and the standard covariant regularization of $\boldsymbol{\Sigma}_0$ and $\boldsymbol{\Sigma}_1$. A simple calculation in the momentum space gives the following expression for $\mathbf{\Sigma}_0$

$$\mathbf{\Sigma}_0(\boldsymbol{p}_2,\,\boldsymbol{p}_1) = -\frac{\alpha}{2\pi}\left[\frac{3}{4}+\frac{1}{2}\ln\left(\frac{\Lambda^2}{\boldsymbol{p}_2^2}\right)\vartheta(\Lambda^2-\boldsymbol{p}_2^2)\right]\hat{p}_2(2\pi)^3\delta(\boldsymbol{p}_2-\boldsymbol{p}_1) \quad , \tag{20}$$

where Λ is the parameter of the regularization, and $\vartheta(x)$ is the step-function. Because of the Dirac equation, $\hat{p}\psi = (-Z\alpha/r)\gamma_0\psi$, the operator $\mathbf{\Sigma}_0$ in the modified Dirac equation can be replaced by

$$\widetilde{\mathbf{\Sigma}}_0(\boldsymbol{p}_2,\,\boldsymbol{p}_1) = \frac{2\alpha(Z\alpha)}{(\boldsymbol{p}_2-\boldsymbol{p}_1)^2}\left[\frac{3}{4}+\frac{1}{2}\ln\left(\frac{\Lambda^2}{\boldsymbol{p}_2^2}\right)\vartheta(\Lambda^2-\boldsymbol{p}_2^2)\right]\gamma^0 \quad , \tag{21}$$

The operator (21) has the same γ-matrix structure as that of $\mathbf{\Sigma}_1$. As a result the sum of $\mathbf{\Sigma}_1$ and $\widetilde{\mathbf{\Sigma}}_0$ is independent of Λ :

$$\begin{aligned}
\mathbf{\Sigma}_{01}(\boldsymbol{p}_2,\,\boldsymbol{p}_1) &= \frac{\alpha(Z\alpha)}{(\boldsymbol{p}_2-\boldsymbol{p}_1)^2}\left\{1+2\int_0^1\!\!\int_0^1\frac{dxdy}{T}\left[x^2y^2(\boldsymbol{p}_2-\boldsymbol{p}_1)^2+(1-x)(x\boldsymbol{p}_1^2+\hat{p}_1\hat{p}_2)\right]\right\}\gamma^0 \quad , \\
T &= y(1-xy)\boldsymbol{p}_2^2+(1-y)(1-x+xy)\boldsymbol{p}_1^2-2xy(1-y)\boldsymbol{p}_1\cdot\boldsymbol{p}_2 \quad .
\end{aligned} \tag{22}$$

The Fourier transform of Eqs. (5),(7) gives the following result for the $s_{1/2}$ wave function in momentum representation

$$\psi(\boldsymbol{p}) = N\frac{4\pi\Gamma(\gamma+1)}{p^{\gamma+2}}\begin{pmatrix}\cos(\pi\gamma/2)\Omega \\ (Z\alpha/\gamma)\sin(\pi\gamma/2)(\boldsymbol{\sigma}\cdot\boldsymbol{n}_p)\Omega\end{pmatrix} \quad , \tag{23}$$

where $\boldsymbol{n}_p = \boldsymbol{p}/p$. Using Eqs. (22), (23), and definition of $F^{(2)}$ and $G^{(2)}$ given in Eq. (9), we find

$$\begin{aligned}
F_s^{(2)} &= \gamma\frac{\cos(\pi\gamma/2)}{\sin(\pi\gamma/2)}\int\frac{p_2^{\gamma+1}}{p_1^{\gamma+2}}\Sigma_{01}(\boldsymbol{p}_2,\boldsymbol{p}_1)\frac{d\boldsymbol{p}_1}{(2\pi)^3}, \\
G_s^{(2)} &= \frac{(\gamma^2-1)\sin(\pi\gamma/2)}{\gamma\cos(\pi\gamma/2)}\int\frac{p_2^{\gamma}}{p_1^{\gamma+3}}(\mathbf{p_1}\cdot\mathbf{p_2})\Sigma_{01}(\boldsymbol{p}_2,\boldsymbol{p}_1)\frac{d\boldsymbol{p}_1}{(2\pi)^3} \quad .
\end{aligned} \tag{24}$$

Evaluation of these integrals and substitution of $F_s^{(2)}$ and $G_s^{(2)}$ in Eq. (13) (see also Eq. (4)) gives

$$\begin{aligned}
\mathcal{A}_{SE}^{(01)} &= -\frac{\alpha(Z\alpha)^2}{2\pi\gamma}\left[\psi(2+\gamma)+\psi(2-\gamma)-\psi(\frac{1+\gamma}{2})-\psi(1-\frac{\gamma}{2})-\frac{1-\gamma}{2(1+\gamma)}\right. \\
&\quad \left.+\,\psi(1/2)-\psi(1)-1+\frac{3}{\gamma^2}+\frac{6}{1-\gamma^2}-\frac{3\pi}{\gamma\sin(\pi\gamma)}\right] \quad .
\end{aligned} \tag{25}$$

Here $\psi(x) = d\ln\Gamma(x)/dx$. The first term of $Z\alpha$-expansion of the function $\mathcal{A}_{SE}^{(01)}$ is $-\alpha(Z\alpha)^2/\pi$. Note that even at $Z = 90$ the exact value of $\mathcal{A}_{SE}^{(01)}$ differs from that given by the first term of the expansion by 10% only.

To find $\mathcal{A}_{SE}^{(n>1)}$ one has to subtract from (18) the contribution (25). To do this we subtract from the integrand in (18) the first term of its $Z\alpha$-expansion at fixed γ. The point is that γ in the integrand comes from the wave function, but not from the self-energy operator. Therefore, doing this subtraction one has to consider γ as an independent parameter. After the subtraction we make substitutions $E = \varepsilon/2\sqrt{\rho}$ and $\rho = \exp(2\tau)$, and take the integral over the azimuth angle of the vector $\boldsymbol{\rho}$. Altogether this gives

$$\begin{aligned}
\mathcal{A}_{SE}^{(n>1)} &= -\frac{2\alpha}{\pi\gamma}\sum_{l=1}^{\infty}\int_{-1}^{1}dx\int_0^{\infty}\!\!\int_0^{\infty}\!\!\int_0^{\infty}\frac{d\varepsilon\,d\tau\,ds}{\mathcal{D}}\,\exp\left[-\varepsilon(\mathcal{D}+\cosh\tau\coth s)\right]\,\Delta \quad , \\
\Delta &= x(1+x)B\cosh(2\gamma\tau)\left\{(Z\alpha)\frac{y}{2}\left[\sin\phi\,I'_{2\nu}(y)-\phi I'_{2l}(y)\right]-(Z\alpha)^2\coth s\left[\cos\phi\,I_{2\nu}(y)-I_{2l}(y)\right]\right\} \\
&\quad +(Z\alpha)(1-x^2)A\cosh(2\gamma\tau)\left[\sin\phi\,I_{2\nu}(y)-\phi\,I_{2l}(y)\right] \\
&\quad +\left[\cos\phi\,I_{2\nu}(y)-I_{2l}(y)\right]\left[-(1+x)B\frac{\varepsilon\gamma\sinh\tau\sinh(2\gamma\tau)}{2\sinh^2 s}+(1-x)A\coth s\,\cosh(2\gamma\tau)\right] \quad .
\end{aligned} \tag{26}$$

Here $\mathcal{D}=\sqrt{\sinh^2\tau+(1-x)/2}$, and $y=\varepsilon/\sinh s$. The leading term of $Z\alpha$-expansion of $\mathcal{A}_{SE}^{(n>1)}$ is

$$-\alpha(Z\alpha)^2(\pi^2-9)/(6\pi).$$

It corresponds to the contribution of the operator $\mathbf{\Sigma}_2$. According to Eq. (19), the leading term of $Z\alpha$-expansion of $\mathcal{A}_{SE}$ reads

$$A_{SE} \;=\; -\frac{\alpha(Z\alpha)^2}{6\pi}(\pi^2-3) \quad . \tag{27}$$

Numerical calculation of integrals in Eq. (26) together with Eq. (25) gives the function $\mathcal{A}_{SE}$ exactly in $Z\alpha$. This function is plotted in Fig. 3

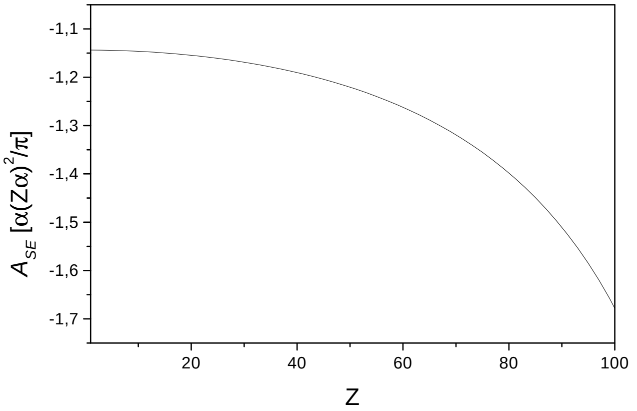

FIG. 3: *The function $\mathcal{A}_{SE}$ calculated in all orders in $Z\alpha$. Value of the function is given in units* $\frac{\alpha(Z\alpha)^2}{\pi}$.

IV. LOGARITHMIC CONTRIBUTION OF THE VERTEX

Let us consider now the logarithmic contribution of the vertex operator (diagram (f) in Fig.1). According to the rules of the diagram technique, the expression for the vertex correction to the matrix element is of the form

$$\begin{aligned} M_f = 2\alpha \int\limits_{-\infty}^{\infty} d\epsilon \iiint d\boldsymbol{r}_1 d\boldsymbol{r}_2 d\boldsymbol{r}_3\, \bar{\psi}_p(\boldsymbol{r}_2)\gamma_\mu \mathcal{G}(\boldsymbol{r}_2,\boldsymbol{r}_3|\, i\epsilon) \\ \times\gamma^0\gamma^5\rho(\boldsymbol{r}_3)\mathcal{G}(\boldsymbol{r}_3,\boldsymbol{r}_1|\, i\epsilon)\gamma^\mu\psi_s(\boldsymbol{r}_1)D(\boldsymbol{r}_2,\boldsymbol{r}_1|i\epsilon)\ , \end{aligned} \tag{28}$$

where, as above, we neglect in (28) the electron mass. We use expansion of the electron Green's function in spherical waves, see Eq. (15). Because of the contact nature of the weak interaction, only the term with angular momentum $j=1/2$ is important in the expansion, this term corresponds to $l=1$ in Eq. (15). Note that $j=1/2$ dominates only in the calculation with logarithmic accuracy. For a calculation of the constant near the logarithm one has to take into account all the partial waves in spite of the contact nature of the weak interaction. Now we calculate only the logarithmic contribution. The logarithmic contribution to the amplitude M_f comes from the region of integration $r_1\sim r_2$, $\lambda_C\gg r_{1,2}\gg r_3\sim r_0$, $\epsilon\sim 1/r_{1,2}$. In this case the parameter s in the integral representation Eq.(15) is of the order of unity, $s\sim 1$, and hence the argument of the Bessel function is small, $y\sim(r_3/r_{1,2})^{1/2}\ll 1$. Expanding

Bessel functions we transform Eq.(15) to the following form

$$
\begin{aligned}
&\mathcal{G}(\boldsymbol{r}_2,\boldsymbol{r}_1|\,i\epsilon) = -\frac{i}{4\pi r_1 r_2\Gamma(2\gamma+1)}\int_0^\infty ds\,\exp\left[\,2iZ\alpha\lambda s\,-\,k(r_2+r_1)\coth s\,\right]\\
&\times\left(\frac{k\sqrt{r_2 r_1}}{\sinh s}\right)^{2\gamma}\Bigg\{[1-(\boldsymbol{\gamma}\boldsymbol{n}_2)(\boldsymbol{\gamma}\boldsymbol{n}_1)]\gamma^0(\gamma\lambda-iZ\alpha\coth s)+[1+(\boldsymbol{\gamma}\boldsymbol{n}_2)(\boldsymbol{\gamma}\boldsymbol{n}_1)]\gamma^0\lambda\\
&-\frac{k(r_2-r_1)}{2\sinh^2 s}(\boldsymbol{\gamma},\boldsymbol{n}_2+\boldsymbol{n}_1)\,-\,(\boldsymbol{\gamma},\boldsymbol{n}_2-\boldsymbol{n}_1)\coth s\Bigg\}\,. \qquad (29)
\end{aligned}
$$

It is convenient to perform integration by parts over s in the term proportional to (r_2-r_1). After that we substitute (29) in equation (28) and take the integral over $\boldsymbol{r}_3$. As a result we get

$$
\begin{aligned}
&M_f = \frac{\alpha\, r_0^{2(\gamma-1)}}{2\pi^2\Gamma^2(2\gamma+1)}\int_0^\infty d\epsilon\iint\frac{d\boldsymbol{r}_1 d\boldsymbol{r}_2}{r_1 r_2}\sum_{\lambda=\pm1}\int_0^\infty\!\!\int_0^\infty ds_1 ds_2\,\exp\left[\,2iZ\alpha\lambda(s_1+s_2)-\epsilon(r_1\coth s_1+r_2\coth s_2)\,\right]\\
&\times\left(\frac{\epsilon^2\sqrt{r_1 r_2}}{\sinh s_1\sinh s_2}\right)^{2\gamma}\,\bar{\psi}_p(\boldsymbol{r}_2)\Bigg\{\gamma^0[1-(\boldsymbol{\gamma}\boldsymbol{n}_1)(\boldsymbol{\gamma}\boldsymbol{n}_2)]\,(1-\coth s_1\coth s_2)+\gamma^0[1+(\boldsymbol{\gamma}\boldsymbol{n}_1)(\boldsymbol{\gamma}\boldsymbol{n}_2)]\\
&\times[\gamma\,(1+\coth s_1\coth s_2)-iZ\alpha\lambda\,(\coth s_1+\coth s_2)]+\lambda(\boldsymbol{\gamma},\boldsymbol{n}_1+\boldsymbol{n}_2)\,(\coth s_1-\coth s_2)\\
&+(\boldsymbol{\gamma},\boldsymbol{n}_1-\boldsymbol{n}_2)\,[\gamma\lambda\,(\coth s_1+\coth s_2)-iZ\alpha\,(\coth s_1\coth s_2+1)]\Bigg\}\gamma^5\psi_s(\boldsymbol{r}_1)\,D(\boldsymbol{r}_2,\boldsymbol{r}_1|i\epsilon)\,. \qquad (30)
\end{aligned}
$$

Then we substitute the photon propagator (17) and the electron wave functions (5), (7), and find the following expression for the relative correction δ_f

$$
\begin{aligned}
\delta_f &= -\frac{\alpha}{8\pi^3\Gamma^2(2\gamma+1)}\int_0^\infty d\epsilon\iint\frac{d\boldsymbol{r}_1 d\boldsymbol{r}_2}{r_1^2 r_2^2}\frac{\exp(-\epsilon R)}{R}\sum_{\lambda=\pm1}\int_0^\infty\!\!\int_0^\infty ds_1 ds_2\,\exp\left[\,2iZ\alpha\lambda(s_1+s_2)\right.\\
&\quad\left.-\epsilon(r_1\coth s_1+r_2\coth s_2)\,\right]\left(\frac{\epsilon^2 r_1 r_2}{\sinh s_1\sinh s_2}\right)^{2\gamma}\mathcal{F}\,,\\
\mathcal{F} &= (1-x^2)(1-\gamma)\,[(1+\gamma)\coth s_1\coth s_2-(1-\gamma)-iZ\alpha\lambda\,(\coth s_1+\coth s_2)]+2(1-x\coth s_1\coth s_2)\,,\\
R &= \sqrt{r_1^2+r_2^2-2xr_1r_2}\quad,\quad x=\boldsymbol{n}_1\cdot\boldsymbol{n}_2\quad. \qquad (31)
\end{aligned}
$$

At the next step we introduce new variables ρ, t, E via the relations $r_1=\rho t$, $r_2=\rho/t$, $\epsilon\sqrt{r_1 r_2}=E$, perform integration over ρ with logarithmic accuracy in limits $r_0<\rho<\lambda_C$, and take integrals over all the angles except of the angle between vectors $\boldsymbol{r}_1$ and $\boldsymbol{r}_2$. This gives the following expression for the contribution of the vertex operator to the function $\mathcal{A}$ defined in Eq.(4):

$$
\begin{aligned}
\mathcal{A}_V &= -\frac{2\alpha}{\pi\Gamma^2(2\gamma+1)}\int_0^\infty dE\int_0^\infty\frac{dt}{t}\int_{-1}^1 dx\,\frac{\exp(-ER)}{R}\sum_{\lambda=\pm1}\int_0^\infty\!\!\int_0^\infty ds_1 ds_2\,\exp\left[\,2iZ\alpha\lambda(s_1+s_2)\,-\right.\\
&\quad\left.-E(t\coth s_1+(1/t)\coth s_2)\,\right]\left(\frac{E^2}{\sinh s_1\sinh s_2}\right)^{2\gamma}\mathcal{F}\,. \qquad (32)
\end{aligned}
$$

Here $R=\sqrt{t^2+1/t^2-2x}$ and $\mathcal{F}$ is defined in (31). A simple integration over E leads to

$$
\begin{aligned}
\mathcal{A}_V &= -\frac{2\alpha\Gamma(4\gamma+1)}{\pi\Gamma^2(2\gamma+1)}\int_0^\infty\frac{dt}{t}\int_{-1}^1\frac{dx}{R}\sum_{\lambda=\pm1}\int_0^\infty\!\!\int_0^\infty\frac{ds_1 ds_2\,\exp[\,2iZ\alpha\lambda(s_1+s_2)]}{(\sinh s_1\sinh s_2)^{2\gamma}}\\
&\quad\times\frac{\mathcal{F}}{[t\coth s_1+(1/t)\coth s_2+R]^{4\gamma+1}}\,. \qquad (33)
\end{aligned}
$$

The last integration which can be performed analytically is the integration over x. The result is rather cumbersome:

$$\begin{aligned}
\mathcal{A}_V \; = \; & -\frac{\alpha\Gamma(4\gamma+1)}{\pi\gamma\Gamma^2(2\gamma+1)}\int_0^\infty \frac{dt}{t}\sum_{\lambda=\pm1}\int_0^\infty\!\!\int_0^\infty \frac{ds_1 ds_2\, \exp[\,2iZ\alpha\lambda(s_1+s_2)]}{(\sinh s_1 \sinh s_2)^{2\gamma}} \\
& \times\Bigg\{\left[\frac{(1-\coth s_1\coth s_2)}{D_-^{4\gamma}}-\frac{(1+\coth s_1\coth s_2)}{D_+^{4\gamma}}\right] \\
& +\frac{1}{4\gamma-1}\left[\frac{|t-1/t|(Q+\coth s_1\coth s_2)}{D_-^{4\gamma-1}}-\frac{(t+1/t)(-Q+\coth s_1\coth s_2)}{D_+^{4\gamma-1}}\right]+ \\
& +\frac{1}{(4\gamma-1)(4\gamma-2)}\left[\frac{Q(3-t^2-1/t^2)+\coth s_1\coth s_2}{D_-^{4\gamma-2}}-\frac{Q(-3-t^2-1/t^2)+\coth s_1\coth s_2}{D_+^{4\gamma-2}}\right]- \\
& -\frac{3Q}{(4\gamma-1)(4\gamma-2)(4\gamma-3)}\left[\frac{|t-1/t|}{D_-^{4\gamma-3}}-\frac{(t+1/t)}{D_+^{4\gamma-3}}\right]- \\
& -\frac{3Q}{(4\gamma-1)(4\gamma-2)(4\gamma-3)(4\gamma-4)}\left[\frac{1}{D_-^{4\gamma-4}}-\frac{1}{D_+^{4\gamma-4}}\right]\Bigg\}\,. \qquad (34)
\end{aligned}$$

The following notation are used:

$$\begin{aligned}
Q \; &= \; (1-\gamma)\left[(1+\gamma)\coth s_1\coth s_2-(1-\gamma)-iZ\alpha\lambda(\coth s_1+\coth s_2)\right], \\
D_- \; &= \; t\coth s_1+(1/t)\coth s_2+|t-1/t|\,,\; D_+=t\coth s_1+(1/t)\coth s_2+(t+1/t)\,. \qquad (35)
\end{aligned}$$

The part of the vertex that is independent of $Z\alpha$ requires the ultraviolet regularization and hence is dependent on the regularization parameter. In fact we have put the regularization parameter to be equal to $1/r_0$. The corresponding Z-independent term in Eq.(34) equals to $\alpha/2\pi$. One should also take into account the term that provides the correct normalization of the total wave function, see e.g. Ref.[27],

$$\begin{aligned}
\delta_N \; = \; & -\alpha\int\limits_{-\infty}^{\infty} d\epsilon\iiint d\boldsymbol{r}_1 d\boldsymbol{r}_2 d\boldsymbol{r}_3\,\bar{\psi}_p(\boldsymbol{r}_2)\gamma_\mu\mathcal{G}(\boldsymbol{r}_2,\boldsymbol{r}_3|\,i\epsilon) \\
& \times\gamma^0\mathcal{G}(\boldsymbol{r}_3,\boldsymbol{r}_1|\,i\epsilon)\gamma^\mu\psi_p(\boldsymbol{r}_1)D(\boldsymbol{r}_2,\boldsymbol{r}_1|i\epsilon) \\
& +(\psi_p\to\psi_s)\;. \qquad (36)
\end{aligned}$$

Straightforward calculation of this contribution with logarithmic accuracy gives $-\alpha\, L/2\pi$. Note that there are no Z-dependent logarithmic terms in (36). As a result the "normalization" contribution cancels out exactly the Z-independent term in $\mathcal{A}_V$. In essence this cancellation is a direct consequence of the Ward identity. The leading term of $Z\alpha$-dependent part of $\mathcal{A}_V$ at $Z\alpha\ll1$ reads

$$\mathcal{A}_V=-\frac{\alpha(Z\alpha)^2}{\pi}\left(\frac{17}{4}-\frac{\pi^2}{3}\right)\quad . \qquad (37)$$

Numerical calculation of integrals in Eq. (34) together with account of the normalization contribution (36) gives the function $\mathcal{A}_V$ exactly in $Z\alpha$. This function is plotted in Fig. 4

Equations (27) and (37) give the final result for $\mathcal{A}$ at $Z\alpha\ll1$

$$\mathcal{A}=\mathcal{A}_{SE}+\mathcal{A}_V=-\frac{\alpha(Z\alpha)^2}{\pi}\left(\frac{15}{4}-\frac{\pi^2}{6}\right)\quad . \qquad (38)$$

The function $\mathcal{A}(Z\alpha)$ with account of all orders in $Z\alpha$ is plotted in Fig. 5

V. LINEAR IN $Z\alpha$ RADIATIVE CORRECTIONS

In the leading $\alpha(Z\alpha)$ approximation, it is convenient to derive the non-logarithmic term of the radiative correction using the effective operator approach, see e. g. Ref. [28]. In this approach the corrections under discussion coincide

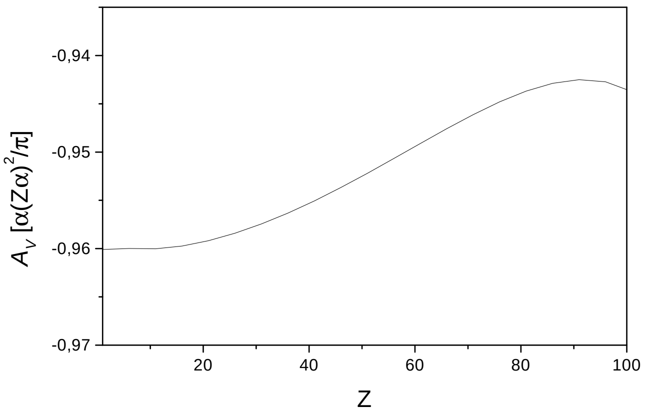

FIG. 4: *The function $\mathcal{A}_V$ calculated in all orders in $Z\alpha$. Value of the function is given in units* $\frac{\alpha(Z\alpha)^2}{\pi}$.

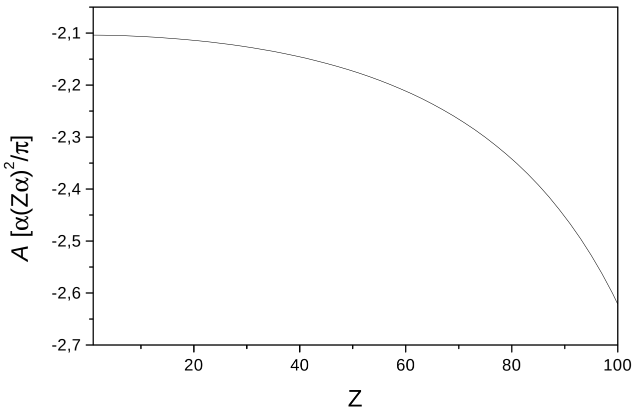

FIG. 5: *The function $\mathcal{A}$ calculated in all orders in $Z\alpha$. Value of the function is given in units* $\frac{\alpha(Z\alpha)^2}{\pi}$.

with those for the $\boldsymbol{\sigma}\cdot\boldsymbol{p}$ structure in the amplitude of low-energy forward scattering. Diagrams for the scattering amplitude are shown in Fig.6. Below we double the contribution of each diagram because of permutation of Z-boson and Coulomb lines. In these amplitudes the momentum $|\boldsymbol{p}|$ of the external electron is small compared to the momentum of the Coulomb quantum, $k \sim m$. Renormalization procedures for the self-energy operator and for the photon vertex operator are standard ones. For the Z-boson vertex we have to set the vertex correction equal to zero at $k = 0$ because as a reference point we use result [13] that is normalized at $k = 0$. To minimize the infrared problems we perform calculations in the Fried-Yennie gauge [23] where the photon propagator is of the form

$$D_{\mu\nu}(q) = \frac{g_{\mu\nu}q^2 + 2q_\mu q_\nu}{(q^2 + i0)^2} \quad . \tag{39}$$

This gauge does not require an introduction of the photon mass for infrared regularization. In this gauge the renormalized self-energy operator has the form [28]

$$\boldsymbol{\Sigma}(p) = -\frac{3\alpha\hat{p}\,(\hat{p}-m)^2}{4\pi m^2(1-\rho)}\left(1 + \frac{\rho}{1-\rho}\ln\rho\right), \tag{40}$$

where $\rho = 1 - p^2/m^2$. Calculating the diagram Fig.6(a) with this self-energy operator we obtain the following contribution to the function $\mathcal{B}$ defined in Eq. (4)

$$\mathcal{B}_a = \frac{5}{4}\alpha(Z\alpha)\,. \tag{41}$$

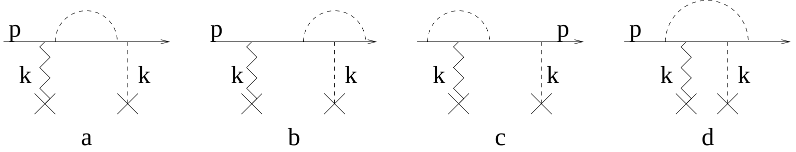

FIG. 6: *Self-energy and vertex radiative corrections to the forward scattering amplitude. The zigzag line denotes Z-boson and the dashed line denotes photon. The cross denotes the nucleus. Contribution of each diagram must be doubled because of permutation of Z-boson and Coulomb lines.*

A straightforward calculation leads to the following expression for the renormalized correction to the photon vertex operator

$$\Lambda_\alpha = \frac{\alpha}{4\pi}\left\{-3\gamma_\alpha\int_0^1 dy\left(\ln[1+\tau y(1-y)]+\frac{1}{2}\right)+\int_0^1 dy\int_0^1\frac{dx}{m^2T}\right. \tag{42}$$
$$\times\left[x^2\left(b^2\gamma_\alpha+2\hat{b}\gamma_\alpha\hat{b}\right)+2x\left(\gamma_\alpha\hat{p}_2\hat{b}+\hat{b}\hat{p}_1\gamma_\alpha-\hat{b}\gamma_\alpha\hat{p}_1-\hat{p}_2\gamma_\alpha\hat{b}+6mb_\alpha\right)+(x-2)\gamma_\mu(\hat{p}_1+m)\gamma_\alpha(\hat{p}_2+m)\gamma_\mu\right]$$
$$\left.+\int_0^1 dy\int_0^1\frac{(1-x)xdx}{m^4T^2}\left[2\hat{b}(\hat{p}_1+m)\gamma_\alpha(\hat{p}_2+m)\hat{b}\right]\right\}.$$

Here the incoming electron has the momentum p_2 and outgoing electron the momentum $p_1 = p_2 + k$,

$$b = [p_1(1-y)+p_2 y]\,,\quad T = x+\tau y(1-xy)+\lambda y(1-x),\quad \tau=\frac{\boldsymbol{k}^2}{m^2},\quad \lambda=\frac{2\boldsymbol{p}\cdot\boldsymbol{k}}{m^2}\ .$$

Performing calculations with this vertex function we find the contribution of the diagram Fig.6(b)

$$\mathcal{B}_b = \alpha(Z\alpha)\left(-\frac{7}{12}-\frac{8}{3}\ln 2\right)\ . \tag{43}$$

The renormilized correction to the Z-boson vertex reads

$$\text{\L}_\alpha = \frac{\alpha}{4\pi}\left\{-\gamma_\alpha\int_0^1 dy\left(3\ln[1+\tau y(1-y)]-\frac{1}{2}\right)+\int_0^1 dy\int_0^1\frac{dx}{m^2T}\right. \tag{44}$$
$$\times\left[x^2\left(b^2\gamma_\alpha+2\hat{b}\gamma_\alpha\hat{b}\right)+2x\left(\gamma_\alpha\hat{p}_2\hat{b}+\hat{b}\hat{p}_1\gamma_\alpha-\hat{b}\gamma_\alpha\hat{p}_1-\hat{p}_2\gamma_\alpha\hat{b}+m(\hat{b}\gamma_\alpha-\gamma_\alpha\hat{b})\right)\right.$$
$$\left.\left.+(-2+x)\gamma_\mu(\hat{p}_1+m)\gamma_\alpha(\hat{p}_2-m)\gamma_\mu\right]+\int_0^1 dy\int_0^1\frac{(1-x)xdx}{m^4T^2}\left[2\hat{b}(\hat{p}_1+m)\gamma_\alpha(\hat{p}_2-m)\hat{b}\right]\right\}\gamma_5.$$

Calculation with this vertex function gives the following contribution of the diagram Fig.6(c)

$$\mathcal{B}_c = \alpha(Z\alpha)\left(\frac{1}{4}-\frac{10}{3}\ln 2\right)\ . \tag{45}$$

The last diagram, Fig.6(d), does not require any renormalization. A straightforward calculation gives

$$\mathcal{B}_d = \alpha(Z\alpha)\left(-\frac{3}{2}+4\ln 2\right)\ . \tag{46}$$

Altogether, the result for the non-logarithmic term in Eq.(4) reads

$$\mathcal{B} = \mathcal{B}_a+\mathcal{B}_b+\mathcal{B}_c+\mathcal{B}_d = -\alpha(Z\alpha)\left(\frac{7}{12}+2\ln 2\right). \tag{47}$$

Thus, according to Eqs. (4), (38), and (47) total relative correction in the leading $Z\alpha$-approximation reads

$$\delta_{ef} \ = \ -\alpha\left[(Z\alpha)\left(\frac{7}{12}+2\ln 2\right)+\frac{(Z\alpha)^2}{\pi}\left(\frac{15}{4}-\frac{\pi^2}{6}\right)\ln(b\lambda_C/r_0)\right]\quad . \tag{48}$$

The curve corresponding to this formula is shown in Fig.7 by the dotted line pnc1. By the dashed line pnc2 we show the correction δ_{ef} calculated with the exact in $Z\alpha$ function $\mathcal{A}$. The solid line pnc in the same Fig.7 shows the total radiative correction to the PNC effect that includes both δ_{ef} and δ_b (Eq.(2), Fig.1(b)). The leading unaccounted contribution in δ_{ef} is of the order of $\sim Z^2\alpha^3/\pi$. For Cs (Z=55) this gives about 5% uncertainty in δ_{ef}.

VI. RADIATIVE CORRECTIONS TO THE FINITE-NUCLEAR-SIZE EFFECT

The radiative shift of the atomic energy levels (Lamb shift) depends on the finite nuclear size. This correction has a very similar structure to that of the PNC radiative correction since the effective sizes of the perturbation sources in both cases are much smaller than λ_C. The self-energy and the vertex corrections to the finite-nuclear-size effect (SEVFNS) for $s_{1/2}$-state have been calculated earlier analytically in order $\alpha(Z\alpha)$ in Refs.[29, 30]. The corrections for $1s_{1/2}$-, $2s_{1/2}$-, and $2p_{1/2}$-states have been calculated numerically exactly in $Z\alpha$ in Refs.[19, 33, 34]. However, the structure of higher in $Z\alpha$ corrections and their logarithmic dependence on the nuclear size has not been understood. We have applied our approach to the SEVFNS problem and found the following expression for the $s_{1/2}$-state relative correction in the leading $Z\alpha$-approximation

$$\Delta_s = -\alpha\left[(Z\alpha)\left(\frac{23}{4} - 4\ln 2\right) + \frac{(Z\alpha)^2}{\pi}\left(\frac{15}{4} - \frac{\pi^2}{6}\right)\ln(b\lambda_C/r_0)\right] \quad . \tag{49}$$

Linear in $Z\alpha$ term agrees with results of Refs. [29, 30]. The correction Δ_s given by Eq. (49) is shown in Fig. 7 by the dotted line fs1. By the dashed line fs2 we show the correction Δ_s calculated with the exact in $Z\alpha$ function $\mathcal{A}$. Results of the computations [19, 20] for $1s$ and $2s$ states are shown by circles and diamonds, respectively. The agreement is excellent.

Note that logarithmic terms ($\ln(b\lambda_C/r_0)$) in δ_{ef} and Δ_s coincide. This statement is valid in all orders in $Z\alpha$. Moreover, the logarithmic term in the SEVFNS correction Δ_p for $p_{1/2}$ state is also equal to that in δ_{ef} and Δ_s. The reason for this equality is very simple. The logarithmic terms come from small distances ($r << \lambda_C$) where the electron mass can be neglected. When the mass is neglected the relative matrix elements for the PNC radiative correction and for SEVFNS are equal.

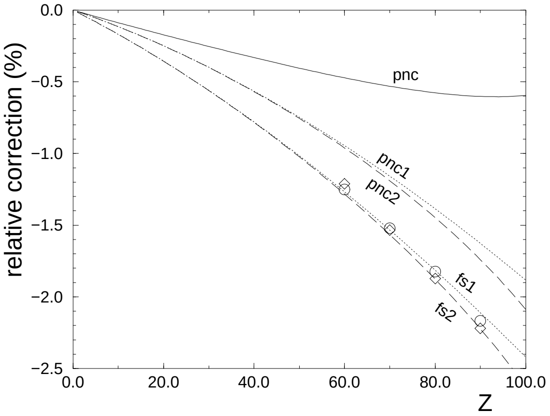

FIG. 7: *Relative radiative corrections (%) for the PNC and for the finite-nuclear-size effects versus the nuclear charge Z. The dotted line pnc1 shows the correction δ_{ef} (Fig.1(e,f)) when both logarithmic and nonlogarithmic terms are calculated in leading in $Z\alpha$ orders, see Eq.(48). The same correction, but with logarithmic term calculated exactly in $Z\alpha$, is shown by the dashed line pnc2. The solid line pnc shows the total radiative correction to the PNC effect that includes both δ_{ef} and δ_b (Eq.(2), Fig.1(b)). The dotted line fs1 shows the finite nuclear size correction Δ_s when both logarithmic and nonlogarithmic terms are calculated in leading in $Z\alpha$ orders, see Eq.(49). The same correction, but with logarithmic term calculated exactly in $Z\alpha$, is shown by the dashed line fs2. Results of computations of Δ_s for $1s$ and $2s$ states [19, 20] are shown by circles and diamonds, respectively.*

The correction Δ_p is calculated in our work [31]. The result reads

$$\Delta_p = -\alpha\left[-\frac{8}{9\pi}\left(\ln\frac{1}{(Z\alpha)^2} + 0.910\right) + 2.75(Z\alpha) + \frac{(Z\alpha)^2}{\pi}\left(\frac{15}{4} - \frac{\pi^2}{6}\right)\ln(b\lambda_C/r_0)\right] \; . \tag{50}$$

Structure of this correction is qualitatively different from that of δ_{ef} and Δ_s, the expansion starts from $\alpha\ln(1/Z\alpha)$ term, while in δ_{ef} and Δ_s it starts from $Z\alpha^2$. This difference is due to the different infrared dynamics, see discussion in [31].

It has been suggested in Ref. [32] that the relation $\delta_{ef} = (\Delta_s + \Delta_p)/2$ is valid. Our results (48), (49), and (50) clearly disagree with this relation. Although, due to accidental compensations, the relation is more or less valid numerically around $Z \approx 57$, we strongly insist that there is no valid justification for the relation. The "derivation" in Ref. [32] is based on an assumption that there is a gauge in which the vertex contributions to δ_{ef}, Δ_s, and Δ_p vanish simultaneously. This assumption is obviously wrong, and this is why the above relation is wrong.

VII. CONCLUSION

Now we can perform a consistent analysis of the experimental data on atomic parity violation since all the contributions are known. In our analysis for Cs we include the theoretical value of the PNC amplitude from Refs. [7, 8, 9, 10]

$$E_{PNC} = 0.908(1 \pm 0.005)\ 10^{-11}\ iea_B(-Q_W/N), \tag{51}$$

as well as the -0.61% correction due to the Breit interaction [12], the -0.85% radiative correction calculated in the present work, the $+0.42\%$ vacuum polarization correction [16, 17], the -0.2% neutron skin correction [35], the -0.08% correction due to the renormalization of Q_W from the atomic momentum transfer $q \sim 30$MeV down to $q = 0$ [17], and the $+0.04\%$ contribution from the electron-electron weak interaction [17]. The theoretical uncertainty from the $Z^2\alpha^3/\pi$ term unaccounted in the present calculation is about $0.05 - 0.1\%$. In Ref. [4] the ratio E_{PNC}/β has been measured with 0.35% accuracy. Here β is the vector transition polarizability. An analysis of the recent data on β has been performed in Ref.[10]. We use the value $\beta = 26.99(5)a_B^3$ obtained in [10]. Combining all these results we obtain the following value of the nuclear weak charge Q_W at zero momentum transfer

$$Cs: \quad Q_W = -72.81 \pm (0.28)_{ex} \pm (0.36)_{theor}. \tag{52}$$

This value agrees with prediction of the standard model, $Q_W = -73.09 \pm 0.03$, see Ref. [5]. We have used the neutron skin correction in our analysis. However, in our opinion, status of this correction is not quite clear because data on the neutron distribution used in Ref. [35] are not quite consistent with data on the neutron distributions obtained from proton scattering, see e. g. Ref. [36].

In the analysis for Tl we have included the theoretical value of the PNC amplitude from Refs. [6], as well as the -0.88% correction due to the Breit interaction [37], the -1.48% radiative correction calculated in the present work, the $+0.90\%$ vacuum polarization correction [17], the -0.2% neutron skin correction, the -0.08% correction due to the renormalization of Q_W from the atomic momentum transfer $q \sim 30$MeV down to $q = 0$ [17], and the $+0.01\%$ contribution from the electron-electron weak interaction [17]. Using these theoretical results we obtain from the data [3] the following value of the nuclear weak charge Q_W at zero momentum transfer

$$Tl: \quad Q_W = -116.8 \pm (1.2)_{ex} \pm (3.4)_{theor}. \tag{53}$$

This agrees with prediction of the standard model, $Q_W = -116.7 \pm 0.1$, see Ref. [5]. Values of the weak charge Q_W obtained in the present work differ a little from that reported in [18]. There are two reasons for the difference, a) in the present work we have used a slightly different value for Cs vector transition polarizability, this value is probably more accurate, b) in the present work calculation of the logarithmic term in the radiative correction is performed exactly in $Z\alpha$, while in [18] we have used only the leading term of $Z\alpha$-expansion.

Concluding, we have calculated the radiative corrections to the effect of atomic parity violation, the corrections are enhanced by the collective electric field of the nucleus . This calculation has allowed us to perform a consistent analysis of the experimental data on the nuclear weak charge. Agreement with the standard model is within 0.6σ.

We would like to thank V. A. Dzuba for helpful discussions. A.I.M gratefully acknowledge the School of Physics at the University of New South Wales for warm hospitality and financial support during a visit.

---

[1] L. M. Barkov and M. S. Zolotorev, JETP Lett., **27**, 357 (1978); M. J. D. MacPherson *et al.*, Phys. Rev. Lett., **67**, 2784 (1991).
[2] D. M. Meekhof *et al.*, Phys. Rev. Lett., **71**, 3442 (1993).
[3] N. H. Edwards *et al.*, Phys. Rev. Lett., **74**, 2654 (1995); P. A. Vetter *et al.*, Phys. Rev. Lett., **74**, 2658 (1995).
[4] C. S. Wood *et al.*, Science **275**, 1759 (1997); S. C. Bennett and C. E. Wieman, Phys. Rev. Lett. **82**, 2484 (1999).
[5] D. E. Groom *et al* Euro. Phys. J. C **15**, 1 (2000).
[6] V. A. Dzuba, V. V. Flambaum, P. G. Silvestrov, and O. P. Sushkov, J. Phys. B **20**, 3297 (1987); Europhys. Lett. **7**, 413 (1988).
[7] V. A. Dzuba, V. V. Flambaum, and O. P. Sushkov, Phys. Lett. **141A**, 147 (1989).
[8] S. A. Blundell, J. Sapirstein, and W. R. Johnson, Phys. Rev. Lett. **65**, 1411 (1990); Phys. Rev. **D45**, 1602 (1992).
[9] M. G. Kozlov, S. G. Porsev, and I. I. Tupitsyn, Phys. Rev. Lett. **86**, 3260 (2001).
[10] V. A. Dzuba, V. V. Flambaum and J. S. M. Ginges, Phys. Rev. D **66**, 076013 (2002); V. A. Dzuba and V. V. Flambaum, Phys. Rev. A **62**, 052101 (2000).
[11] A. Derevianko, Phys. Rev. Lett. **85**, 1618 (2000).
[12] V. A. Dzuba, C. Harabati, W. R. Johnson, and M. S. Safronova, Phys. Rev. A **63**, 044103 (2001).

[13] W. J. Marciano and A. Sirlin, Phys. Rev. D **27**, 552 (1983).
[14] W. J. Marciano and J. L. Rosner, Phys. Rev. Lett. **65**, 2963 (1990).
[15] O. P. Sushkov, Phys. Rev. A **63**, 042504 (2001);
[16] W. R. Johnson, I. Bednyakov and G. Soff, Phys. Rev. Lett. **87**, 233001 (2001).
[17] A. I. Milstein and O. P. Sushkov, Phys. Rev. A **66**, 022108 (2002).
[18] A. I. Milstein, O. P. Sushkov and I. S. Terekhov, Phys. Rev. Letters, to appear; hep-ph/0208227.
[19] K. T. Cheng, W. R. Johnson, and J. Sapirstein, Phys. Rev. A **47**, 1817 (1993).
[20] W. R. Johnson and G. Soff, At. Data Nuc. Data Tables **33**, 405 (1985).
[21] *Parity nonconservation in atomic phenomena*, I. B. Khriplovich, Gordon and Breach, 1991.
[22] C. J. Horowitz, S. J. Pollock, P. A. Souder, and R. Michaels, Phys. Rev. C **63**, 025501 (2001).
[23] H. M. Fried and D. R. Yennie, Phys. Rev. **112**, 1391 (1958).
[24] V. B. Berestetskii, E. M. Lifshitz, and L. P. Pitaevskii, *Relativistic quantum theory* (Pergamon Press, Oxford, 1982).
[25] A.I. Milstein, V.M. Strakhovenko, Phys. Lett. A **90**, 447 (1982).
[26] R. N. Lee and A. I. Milstein, Phys. Lett. A **189**, 72 (1994).
[27] K. Pachucki, Phys. Rev. A **54**, 1994 (1996).
[28] M. I. Eides, H. Grotch, and V. A. Shelyuto, Phys. Rep. **342**, 63 (2001).
[29] K. Pachucki, Phys. Rev. A **48**, 120 (1993).
[30] M. I. Eides , H. Grotch, Phys. Rev. A **56**, R2507 (1997).
[31] A. I. Milstein, O. P. Sushkov and I. S. Terekhov, physics/0212018.
[32] M. Yu. Kuchiev and V. V. Flambaum, hep-ph/0206124.
[33] S. A. Blundell, Phys. Rev. A **46**, 3762 (1992).
[34] I. Lindgren, H. Persson, S. Salomonson, A. Ynnerman, Phys. Rev. A **47**, 4555 (1993).
[35] A. Derevianko, Phys. Rev. A **65**, 012106 (2002);
[36] G. D. Alkhazov *et al*, Sov. J. Nucl. Phys. **26**, 357 (1977).
[37] We found this value by rescaling the Breit correction for Cs [12], see discussion in Refs. [15, 17].